

# Modeling the Impact of Toxicants on a Plankton-Fish System with Gompertz Growth Function

Raveendra Babu Annavarapu, Kavita Makwana, and Bhanu Pratap Singh Jadon



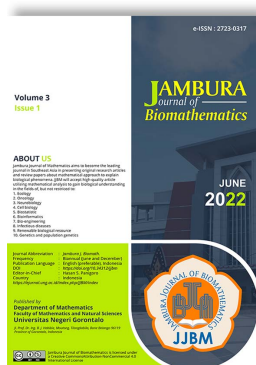
Volume 6, Issue 2, Pages 129–141, June 2025

Received 2 March 2025, Revised 20 June 2025, Accepted 23 June 2025, Published Online 29 June 2025

To Cite this Article : R. B. Annavarapu, K. Makwana, and B. P. S. Jadon, "Modeling the Impact of Toxicants on a Plankton-Fish System with Gompertz Growth Function", *Jambura J. Biomath.*, vol. 6, no. 2, pp. 129–141, 2025, <https://doi.org/10.37905/jjbm.v6i2.30824>

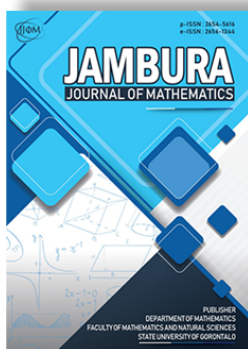
© 2025 by author(s)

## JOURNAL INFO • JAMBURA JOURNAL OF BIOMATHEMATICS



Homepage	: <a href="http://ejurnal.ung.ac.id/index.php/JJBM/index">http://ejurnal.ung.ac.id/index.php/JJBM/index</a>
Journal Abbreviation	: Jambura J. Biomath.
Frequency	: Quarterly (March, June, September and December)
Publication Language	: English
DOI	: <a href="https://doi.org/10.37905/jjbm">https://doi.org/10.37905/jjbm</a>
Online ISSN	: 2723-0317
Editor-in-Chief	: Hasan S. Panigoro
Publisher	: Department of Mathematics, Universitas Negeri Gorontalo
Country	: Indonesia
OAI Address	: <a href="http://ejurnal.ung.ac.id/index.php/jjbm/oai">http://ejurnal.ung.ac.id/index.php/jjbm/oai</a>
Google Scholar ID	: XzYgeKQAAAAJ
Email	: <a href="mailto:editorial.jjbm@ung.ac.id">editorial.jjbm@ung.ac.id</a>

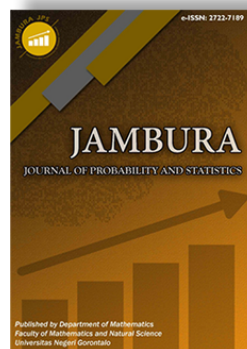
## JAMBURA JOURNAL • FIND OUR OTHER JOURNALS



Jambura Journal of Mathematics



Jambura Journal of Mathematics Education



Jambura Journal of Probability and Statistics



EULER : Jurnal Ilmiah Matematika, Sains, dan Teknologi

# Modeling the Impact of Toxicants on a Plankton-Fish System with Gompertz Growth Function

Raveendra Babu Annavarapu<sup>1</sup> , Kavita Makwana<sup>2,\*</sup> , and Bhanu Pratap Singh Jadon<sup>3</sup>

<sup>1</sup>Department of Information & technology, Prestige Institute of Management and Research, Gwalior 474020, India

<sup>2,3</sup>Department of Mathematics, S.M.S. Govt. Model Science College, Gwalior 474009, India

## ARTICLE HISTORY

Received 2 March 2025

Revised 20 June 2025

Accepted 23 June 2025

Published 29 June 2025

## KEYWORDS

Hopf-bifurcation

Gompertz growth

Prey refuge

Beddington-DeAngelis

Stability

**ABSTRACT.** This study develops a mathematical model to investigate the dynamics of an aquatic ecosystem, incorporating key ecological features such as Gompertz growth, prey refuge, Holling Type II predation, and the Beddington-DeAngelis functional response. The primary objective is to analyze the effects of toxicant accumulation and population interactions on ecosystem stability.

Analytical techniques, including the Jacobian matrix, Routh-Hurwitz criteria, and Lyapunov functions—are employed to examine equilibrium points, stability conditions, and bifurcation behavior. A Hopf bifurcation is observed when the carrying capacity  $K$  exceeds a critical threshold, indicating a transition from stable to oscillatory behavior. Intraspecific competition among fish is found to dampen chaotic dynamics, thereby enhancing system stability.

Numerical simulations confirm the theoretical findings and highlight that increased toxicant levels disrupt energy flow through the food chain, causing population decline. These results underscore the importance of ecological regulation in preserving ecosystem balance and mitigating the impact of environmental stressors.



This article is an open access article distributed under the terms and conditions of the Creative Commons Attribution-NonCommercial 4.0 International License. *Editorial of JJBM:* Department of Mathematics, Universitas Negeri Gorontalo, Jln. Prof. Dr. Ing. B. J. Habibie, Bone Bolango 96554, Indonesia.

## 1. Introduction

The dynamics of plankton-fish interactions have been the subject of several studies, with special focus on the roles played by zooplankton and phytoplankton. Kaur et al. [1] investigated the effects of zooplankton disease and environmental toxicity on harvesting strategies using a phytoplankton-zooplankton model. They found that the optimal collecting techniques for these planktonic species were significantly influenced by both criteria. Panja used a phytoplankton-zooplankton-fish model to study how fear affected fish and zooplankton harvesting. The findings demonstrated that fear-induced behavioral alterations in fish and zooplankton harvesting can lead to complex dynamics, including system bifurcations and stability switches [2]. These factors have the potential to upset the system and result in complex population dynamics and oscillatory behaviors among fish, zooplankton, and phytoplankton, according to Thakur et al.'s analysis of plankton-fish dynamics, which considered top predator interference and multiple gestation delays [3].

Several studies have examined the effects of toxicants on population dynamics using mathematical models. A three-species food chain model with top predator intervention in a toxicant environment was studied by Babu et al. [4]. They showed that toxicants reduce prey's development rate and carrying capacity, which may lead to ecological instability. Sabastine et al. [5] found that high levels of external toxicants can lead to species extinction and adversely affect population persistence in their study of the impacts of these substances on competitive set-

tings. Functional responses are crucial in predator-prey models. While the Holling Type-II response tracks saturation effects, the Beddington-DeAngelis response accounts for predator interference. System stability is demonstrated to be enhanced by predator interference (Zhang et al. [6], Shao and Kong [7], Meng and Wang [8]). Rahmi et al. [9] found bistability and complex patterns, whereas Yu and Chen [10] showed that mutual interference enhances species cohabitation. This study emphasizes the significance of functional responses in shaping population dynamics under ecological pressures. Mukherjee et al. [11] found that the presence of toxic prey significantly affects predator dynamics, and incorporating imprecise (interval) parameters provides a more realistic understanding of how toxicity and harvesting influence the stability and behavior of the ecosystem. Zhu and Xu [12] found that toxicants can induce Turing–Hopf bifurcations, destabilize the system, create complex spatial patterns, and even lead to species extinction.

Furthermore, prey refuge plays a crucial role in preserving predator-prey dynamics by offering protection to a segment of the prey population. It has been demonstrated that prey refuge alters equilibrium densities and enhances population stability. Majeed and Naji [13] found that prey refuge improves system stability, while Lajmire et al. [14] showed that it can result in bifurcation phenomena because of environmental stressors. Both prey distribution and prey refuge have a significant influence on population stability and persistence (Berezovskaya et al. [15]). The growth dynamics of primary producers are crucial for ecosystem modeling since numerous growth functions are used to explain population regulation under environmental stressors. Misra and

\*Corresponding Author.

Babu [16, 17] used the logistic growth function to show how toxicants reduce prey's carrying capacity and growth rate, which impacts a species' ability to persist. Santra [18] employed the  $\theta$ -logistic growth function, which provides a more flexible framework for population regulation with varied growth rates. However, Ahmed and Almatrafi [19] applied the Gompertz growth function to herd behavior and demonstrated that it results in Neimark-Sacker bifurcation and quasi-periodic oscillations. Rana [20] also employed the Gompertz growth function, demonstrating how it leads to flip bifurcation and Neimark-Sacker bifurcation, which lead to complex predator-prey dynamics.

Bifurcation analysis, particularly Hopf bifurcation, must be thoroughly understood in order to comprehend stability transitions in predator-prey systems. It is advantageous to look into how ecological elements like toxicant concentration, fear effects, and predation rates affect population dynamics. Rising toxicant concentrations destabilize the system and create Hopf bifurcation, which results in population oscillations, according to Liu et al. [21], who studied a fractional-order predator-prey model with toxic injections and fear effects. Bosi and Desmarchelier [22] proposed a general framework for detecting local bifurcations in three- and four-dimensional systems using Jacobian matrix minors. This approach provides information on both codimension-one and codimension-two bifurcations with environmental implications. In their study of a predator-prey model, Wang et al. [23] showed that a critical parameter  $d$  governs the system's stability and that transcritical, saddle-node, and Hopf bifurcations, which result in periodic oscillations, occur when it crosses its critical threshold. Makwana et al. [24] studied the bifurcation dynamics of a prey-predator system with toxicants and found that increasing the predation saturation parameter led to Hopf and period-doubling bifurcations, causing transitions from stability to oscillations and chaos. Their results also showed that higher toxicant uptake could restore stability by suppressing population growth. Cong et al. [25] investigated a three-species food chain model with the fear effect and showed that the system undergoes Hopf bifurcation, resulting in periodic population cycles. The fear effect significantly impacts system stability by changing prey behaviour, which can lead to oscillations in the populations of all species.

Although several studies have explored toxicant effects [4, 5, 12], functional responses [6–10], prey refuge [13–15], and various growth dynamics [16–20] individually, there remains a gap in the literature regarding integrated models that simultaneously consider Gompertz growth, prey refuge, Holling Type II and Beddington-DeAngelis functional responses, and toxicant accumulation. Such integration is essential for accurately capturing the multi-layered dynamics of aquatic ecosystems. This study aims to bridge this gap by formulating a comprehensive model that combines these ecological factors, thereby providing a deeper understanding of species persistence, stability, and bifurcation behavior under environmental stress.

## 2. Model Formulation

Understanding the complex interactions between different species in an aquatic ecosystem is crucial for ecological balance and sustainability. In this study, we develop a dynamical system that models the interplay between Phytoplankton ( $P$ ), Zooplank-

ton ( $Z$ ), Fish ( $F$ ), and a Toxicant ( $T$ ). Our model integrates key ecological principles such as prey refuge, Holling Type II predation, Beddington-DeAngelis functional response, and toxicant effects to capture real-world dynamics effectively.

### 2.1. Phytoplankton Dynamics: The Base of the Food Chain

Phytoplankton, the primary producers, exhibit Gompertz growth, which accounts for limited resource availability:

$$\frac{dP}{dt} = rP \ln\left(\frac{K}{P}\right) - \frac{a_1(1-\rho)PZ}{1+b_1P} - d_1P - \tau PT.$$

1. **Intrinsic Growth & Carrying Capacity:** The Gompertz term  $rP \ln\left(\frac{K}{P}\right)$  ensures controlled growth, where  $r$  is the intrinsic growth rate and  $K$  is the carrying capacity of phytoplankton.
2. **Predation by Zooplankton:** Zooplankton consume phytoplankton following a Holling Type II functional response, where  $a_1$  is the predation rate and  $b_1$  is the handling time parameter.
3. **Toxicant Impact:** The term  $-\tau PT$  accounts for the negative effects of pollutants, where  $\tau$  represents the toxicant impact coefficient.
4. **Mortality & Prey Refuge:** A fraction  $\rho$  of phytoplankton escapes predation, and  $d_1$  represents the natural mortality rate of phytoplankton.

### 2.2. Zooplankton Dynamics: The Primary Consumers

Zooplankton thrive by feeding on phytoplankton but are preyed upon by fish:

$$\frac{dZ}{dt} = \frac{a_2(1-\rho)PZ}{1+b_1P} - \frac{a_3ZF}{1+b_2Z+c_2F} - d_2Z - e_1Z^2.$$

1. **Consumption of Phytoplankton:** Governed by Holling Type II functional response, where  $a_2$  represents the predation rate on phytoplankton.
2. **Predation by Fish:** Modeled using the Beddington-DeAngelis response, where  $a_3$  is the predation rate,  $b_2$  is the handling time, and  $c_2$  represents predator interference.
3. **Natural Mortality & Competition:** Zooplankton experience mortality at rate  $d_2$ , and  $e_1Z^2$  ensures stability at high densities due to intraspecific competition.

### 2.3. Fish Dynamics: The Top Predators

Fish depend on zooplankton as their primary food source:

$$\frac{dF}{dt} = \frac{a_4ZF}{1+b_2Z+c_2F} - d_3F - e_2F^2.$$

1. **Predation on Zooplankton:** Follows a Beddington-DeAngelis functional response, where  $a_4$  represents the predation rate on zooplankton.
2. **Mortality & Overcrowding:** Fish experience a natural mortality rate  $d_3$ , while  $e_2F^2$  accounts for competition among fish.

### 2.4. Toxicant Dynamics: The Silent Threat

The toxicant concentration in the ecosystem is affected by external sources and biological interactions:

$$\frac{dT}{dt} = S - d_4T + \gamma PT.$$

1. External Input: The term  $S$  represents pollution entering the system.
2. Natural Decay: The term  $-d_4T$  represents toxicant reduction due to natural degradation, where  $d_4$  is the decay rate.
3. Phytoplankton Influence: Interaction with phytoplankton ( $\gamma PT$ ) may indicate bioaccumulation or biotransformation, where  $\gamma$  is the interaction coefficient.

### 2.5. Complete Model Representation with Initial Conditions

To simulate the ecosystem, we solve the following system of equations:

$$\frac{dP}{dt} = rP \ln \left( \frac{K}{P} \right) - \frac{a_1(1-\rho)PZ}{1+b_1P} - d_1P - \tau PT, \quad (1)$$

$$\frac{dZ}{dt} = \frac{a_2(1-\rho)PZ}{1+b_1P} - \frac{a_3ZF}{1+b_2Z+c_2F} - d_2Z - e_1Z^2, \quad (2)$$

$$\frac{dF}{dt} = \frac{a_4ZF}{1+b_2Z+c_2F} - d_3F - e_2F^2, \quad (3)$$

$$\frac{dT}{dt} = S - d_4T + \gamma PT, \quad (4)$$

with initial conditions:

$$P(0) = P_0 > 0, \quad Z(0) = Z_0 > 0, \quad F(0) = F_0 > 0, \\ T(0) = T_0 > 0.$$

### 2.6. Biological Justification for Gompertz Growth

The Gompertz growth function is adopted instead of the logistic model due to its ability to better represent the decelerating growth of phytoplankton under toxicant stress. Its nonlinear structure captures more realistic dynamics and plays a key role in determining the conditions for Hopf bifurcation, making it well-suited for analyzing stability transitions in polluted aquatic systems.

In addition to its mathematical advantages, the Gompertz growth function has been supported in ecological studies for modeling primary producers under environmental stress [19, 20]. Its gradual slowing of growth aligns with empirical observations of phytoplankton responses to increasing toxicant levels, where growth is more strongly inhibited at higher densities. Therefore, the Gompertz model offers both biological realism and analytical tractability for capturing population regulation in polluted aquatic systems.

### 2.7. Biological Justification for Functional Responses

In this model, the interaction between phytoplankton and zooplankton is represented using the Holling Type II functional response, which captures the saturating feeding behavior commonly observed in herbivorous zooplankton. As prey density increases, the consumption rate rises rapidly but levels off due to handling time limitations. For the fish-zooplankton interaction, the Beddington-DeAngelis response is used to reflect both prey-dependent predation and the effect of predator interference. This formulation is biologically appropriate for fish populations, where competition, territorial behavior, and interference among predators can significantly influence feeding efficiency at higher densities.

### 3. Boundedness of Model

In this section, we establish the boundedness of solutions using the Comparison Theorem to ensure biological feasibility. By constructing suitable differential inequalities, we derive explicit upper bounds for each state variable, confirming that the system remains within a positively invariant region  $\Omega$ . This guarantees that all solutions stay uniformly bounded for  $t \geq 0$ , ensuring the model's validity for long-term analysis.

**Theorem 1.** Let  $(P(t), Z(t), F(t), T(t))$  be a non-negative solution of Model with positive initial conditions. Then, all solutions remain uniformly bounded for all  $t \geq 0$  and ultimately enter a positively invariant compact region  $\Omega$  defined as:

$$\Omega = \{(P, Z, F, T) \in R_+^4 : P \leq K, Z \leq Z_{\max}, F \leq F_{\max}, T \leq T_{\max}\},$$

where,

$$Z_{\max} = \frac{M_Z - d_2}{e_1}, \quad F_{\max} = \frac{A_F}{e_2}, \quad T_{\max} = \frac{S}{\gamma K}, \\ M_Z = \frac{a_2(1-\rho)K}{1+b_1K}, \quad A_F = \frac{a_4(M_Z - d_2)}{e_1c_2} - d_3.$$

*Proof.* From eq. (1), ignoring the negative terms, we approximate,

$$\frac{dP}{dt} \leq rP \ln \left( \frac{K}{P} \right).$$

By solving, the differential equation, we obtain

$$-\ln \left( \ln \left( \frac{K}{P} \right) \right) \leq rt + C, \\ P \leq Ke^{-e^{-rt-C}}.$$

Taking the limit as  $t \rightarrow \infty$ , we obtain

$$P(t) \leq K.$$

This confirms that  $P(t)$  is bounded.

From eq. (2), we approximate,

$$\frac{dZ}{dt} \leq \frac{a_2(1-\rho)PZ}{1+b_1P} - d_2Z - e_1Z^2.$$

Since  $P(t) \leq K$ , define,

$$M_Z = \frac{a_2(1-\rho)K}{1+b_1K}.$$

Then,

$$\frac{dZ}{dt} \leq M_Z Z - d_2Z - e_1Z^2.$$

Solving this Riccati equation, we obtain

$$Z \leq \frac{M_Z - d_2}{e_1(Ce^{-(M_Z-d_2)t} + 1)}.$$

Taking the limit as  $t \rightarrow \infty$ , we obtain

$$Z(t) \leq \frac{M_Z - d_2}{e_1} = Z_{\max}.$$



This confirms that  $Z(t)$  is bounded.

From eq. (3), we approximate,

$$\frac{dF}{dt} \leq A_F F - e_2 F^2,$$

where

$$A_F = \frac{a_4(M_Z - d_2)}{e_1 c_2} - d_3.$$

Using partial fraction, integrating and solving, we obtain

$$F \leq \frac{A_F e^{A_F^2 t + C A_F}}{1 + e^{A_F^2 t + C A_F} e_2}.$$

Taking the limit as  $t \rightarrow \infty$ , we obtain

$$F(t) \leq \frac{A_F}{e_2} = F_{\max}.$$

This confirms that  $F(t)$  is bounded.

From eq. (4), we approximate,

$$\frac{dT}{dt} \leq S + \gamma K T,$$

By solving this, we get,

$$T \leq \frac{S}{\gamma K} + C e^{\gamma K T}.$$

For boundedness, choosing  $C \leq 0$ , we conclude

$$T \leq \frac{S}{\gamma K} = T_{\max}.$$

This confirms that  $T(t)$  is bounded.

Since all variables are bounded, the solutions remain in the compact region  $\Omega$ , proving that the system is ultimately bounded. This completes the proof.  $\square$

#### 4. Existence of Equilibrium Points

This study examines the existence of equilibrium points in a system involving phytoplankton  $P$ , zooplankton  $Z$ , fish  $F$ , and a toxicant  $T$ . We consider three possible equilibrium states:

1.  $E_1(P, 0, 0, T)$ : Only phytoplankton and the toxicant are present.
2.  $E_2(P, Z, 0, T)$ : Phytoplankton and zooplankton coexist, but fish are absent.
3.  $E_3(P, Z, F, T)$ : All species coexist in the system.

By applying equilibrium existence theorems, we establish conditions that ensure each equilibrium is biologically meaningful ( $P, Z, F, T > 0$ ). These findings help in understanding species survival and the influence of toxicants on ecological balance.

**Theorem 2.** Equilibrium point  $E_1(P, 0, 0, T)$  exists if  $d_4 > \gamma P$ .

*Proof.* From eq. (1)

$$r \ln \left( \frac{K}{P} \right) - d_1 - \tau T = 0.$$

After solving for  $P$ , we obtain,

$$P = K e^{\frac{-(d_1 + \tau T)}{r}}.$$

Since exponential function is always positive,  $P > 0 \forall K, r > 0$  and finite  $d_1 + \tau T$ .

Now, from eq. (4),

$$-d_4 T + \gamma P T = 0.$$

After solving for  $T$ , we obtain,

$$T = \frac{S}{d_4 - \gamma P}.$$

$T > 0$  if  $d_4 > \gamma P$ .  $\square$

**Remark 1.** The phytoplankton population  $P$  is negatively impacted by increasing toxicant levels  $T$ , as described by  $P = K e^{\frac{-(d_1 + \tau T)}{r}}$ . While  $P$  remains positive as long as  $T$  is finite, higher concentrations of the toxicant lead to a reduction in phytoplankton growth.

**Remark 2.** The toxicant concentration  $T$  is determined by the phytoplankton population  $P$ , given by  $T = \frac{S}{d_4 - \gamma P}$ . For  $T$  to stay positive, the condition  $d_4 > \gamma P$  must be satisfied, meaning that if  $P$  becomes too large,  $T$  would become negative, which is physically unrealistic.

**Theorem 3.** Equilibrium point  $E_2(P, Z, 0, T)$  exists if  $d_4 > \gamma P$  and  $a_2(1 - \rho)P > d_2(1 + b_1 P)$ .

*Proof.* From eq. (1)

$$r \ln \left( \frac{K}{P} \right) - \frac{a_1(1 - \rho)Z}{1 + b_1 P} - d_1 - \tau T = 0.$$

After solving for  $P$ , we obtain,

$$P = K e^{-\left( \frac{a_1(1 - \rho)Z}{\tau(1 + b_1 P)} + \frac{(d_1 + \tau T)}{r} \right)}.$$

Since exponential function is always positive, hence  $P > 0$  always.

Now, from eq. (2),

$$\frac{a_2(1 - \rho)P}{1 + b_1 P} - d_2 - e_1 Z = 0.$$

After solving for  $Z$ , we obtain,

$$Z = \frac{1}{e_1} \left( \frac{a_2(1 - \rho)P}{(1 + b_1 P)} - d_2 \right).$$

$Z > 0$  if  $a_2(1 - \rho)P > d_2(1 + b_1 P)$ .

This implies that zooplankton can only survive when the term involving the phytoplankton population  $P$  is large enough to overcome the natural death rate and other limiting factors.

Now, from eq. (4),

$$S - d_4T + \gamma PT = 0.$$

After solving for  $T$ , we obtain,

$$T = \frac{S}{d_4 - \gamma P}.$$

$T > 0$  if  $d_4 > \gamma P$ .  $\square$

**Theorem 4.** Equilibrium point  $E_3(P, Z, F, T)$  exists if  $d_4 > \gamma P$ ,  $(1 + b_2)d_3 < a_4Z$  and  $(a_3 + c_2d_2)F + d_2 < f(P)$ , where  $f(P) = \frac{a_2(1-\rho)P}{1+b_1P}$

*Proof.* From eq. (1)

$$r \ln \left( \frac{K}{P} \right) - \frac{a_1(1-\rho)Z}{1+b_1P} - d_1 - \tau T = 0.$$

After solving for  $P$ , we obtain,

$$P = Ke^{-\left( \frac{a_1(1-\rho)Z}{r(1+b_1P)} + \frac{(d_1+\tau T)}{r} \right)}.$$

Since exponential function is always positive, hence  $P > 0$  always.

Now, from eq. (2),

$$\begin{aligned} \frac{a_2(1-\rho)P}{1+b_1P} - \frac{a_3F}{1+b_2Z+c_2F} - d_2 - e_1Z &= 0, \\ f(P) - \frac{a_3F}{1+b_2Z+c_2F} - d_2 - e_1Z &= 0, \end{aligned}$$

where

$$f(P) = \frac{a_2(1-\rho)P}{1+b_1P}.$$

After solving for  $Z$ , we obtain the quadratic equation,

$$0 = b_2e_1Z^2 + (b_2d_2 + e_1 + c_2e_1F)Z + (d_2 - f(P) + (a_3 + c_2d_2)F).$$

This equation has one positive root if  $(a_3 + c_2d_2)F + d_2 < f(P)$ .

Now, from eq. (3),

$$\frac{a_4Z}{1+b_2Z+c_2F} - d_3 - e_2F = 0.$$

After solving for  $F$ , we obtain the quadratic equation,

$$e_2c_2F^2 + (e_2 + c_2d_3 + b_2e_2Z)F + ((1+b_2)d_3 - a_4Z) = 0.$$

This equation has one positive root if  $(1+b_2)d_3 < a_4Z$ .

Now, from eq. (4),

$$S - d_4T + \gamma PT = 0.$$

After solving for  $T$ , we obtain,

$$T = \frac{S}{d_4 - \gamma P}.$$

$T > 0$  if  $d_4 > \gamma P$ .  $\square$

## 5. Local Stability

This section examines the local stability of equilibrium points in the system involving phytoplankton ( $P$ ), zooplankton ( $Z$ ), fish ( $F$ ) and a toxicant ( $T$ ). To determine stability, we compute the Jacobian matrix, which represents the system's linearized behavior around equilibrium points. The Jacobian matrix is given by:

$$J = \begin{bmatrix} A_{11} & -\frac{a_1(1-\rho)P}{(1+b_1P)} & 0 & -\tau P \\ \frac{a_2(1-\rho)Z}{(1+b_1P)^2} & A_{22} & \frac{-a_3Z(1+b_2Z)}{(1+b_2Z+c_2F)^2} & 0 \\ 0 & \frac{a_4F(1+c_2F)}{(1+b_2Z+c_2F)^2} & A_{33} & 0 \\ \gamma T & 0 & 0 & \gamma P - d_4 \end{bmatrix},$$

where

$$\begin{aligned} A_{11} &= r \ln \left( \frac{K}{P} \right) - \frac{a_1(1-\rho)Z}{(1+b_1P)} - \tau T - r - d_1, \\ A_{22} &= \frac{a_3b_2ZF}{(1+b_2Z+c_2F)^2} + \frac{a_2(1-\rho)P}{(1+b_1P)} - \frac{a_3F}{(1+b_2Z+c_2F)} \\ &\quad - 2e_1Z - d_2, \\ A_{33} &= \frac{a_4Z}{(1+b_2Z+c_2F)} - \frac{a_4c_2ZF}{(1+b_2Z+c_2F)^2} - 2e_2F - d_3. \end{aligned}$$

The stability of an equilibrium point is determined by analyzing the eigenvalues of  $J$ . If all eigenvalues have negative real parts, the equilibrium is locally asymptotically stable, meaning small perturbations will decay over time, and the system will return to equilibrium.

**Theorem 5.** The Equilibrium point  $E_1(P, 0, 0, T)$  is locally asymptotically stable if it satisfy the following conditions:

$$\begin{aligned} a_2(1-\rho)P &< d_2(1+b_1P), \\ r \ln \left( \frac{K}{P} \right) + \gamma P &< r + d_1 + d_4 + \tau T, \\ 0 &< \left( r \ln \left( \frac{K}{P} \right) - r - d_1 \right) (\gamma P - d_4) + \tau d_4 T. \end{aligned}$$

*Proof.* Jacobian matrix of Equilibrium point  $E_1(P, 0, 0, T)$  is given by:

$$J = \begin{bmatrix} r \ln \left( \frac{K}{P} \right) - \tau T - r - d_1 & -\frac{a_1(1-\rho)P}{(1+b_1P)} & 0 & -\tau P \\ 0 & \frac{a_2(1-\rho)P}{(1+b_1P)} - d_2 & 0 & 0 \\ 0 & 0 & -d_3 & 0 \\ \gamma T & 0 & 0 & \gamma P - d_4 \end{bmatrix}.$$

Here,

$$\begin{aligned} \lambda_3 &= -d_3 < 0, \\ \lambda_2 &= \frac{a_2(1-\rho)P}{(1+b_1P)} - d_2, \end{aligned}$$

$\lambda_2 < 0$  if  $a_2(1-\rho)P < d_2(1+b_1P)$ . And other two eigen values are given by the following quadratic equation:

$$\lambda^2 + A_1\lambda + B_1 = 0, \quad (5)$$

where

$$A_1 = -r \ln \left( \frac{K}{P} \right) + \tau T - \gamma P + r + d_1 + d_4,$$

$$B_1 = \left( r \ln \left( \frac{K}{P} \right) - r - d_1 \right) (\gamma P - d_4) + \tau d_4 T.$$

According to the Routh-Hurwitz criterion, the polynomial equation is asymptotically stable if it satisfies the conditions:  $A_1, B_1 > 0$ .

- i.  $A_1 > 0$  if  $r \ln \left( \frac{K}{P} \right) + \gamma P < r + d_1 + d_4 + \tau T$ ,
- ii.  $B_1 > 0$  if  $\left( r \ln \left( \frac{K}{P} \right) - r - d_1 \right) (\gamma P - d_4) + \tau d_4 T > 0$ .

□

**Remark 3.** The result of Theorem 5 implies that if the phytoplankton growth is limited and zooplankton cannot invade (due to insufficient feeding efficiency or high death rates), the ecosystem stabilizes at a state where only phytoplankton and toxicant persist. Biologically, this reflects a collapse of the food chain where toxicant stress and lack of viable trophic transfer prevent higher species from surviving.

**Theorem 6.** The Equilibrium point  $E_2$  is locally asymptotically stable under certain conditions.

*Proof.* Jacobian matrix of Equilibrium point  $E_2(P, Z, 0, T)$  is given by:

$$J = \begin{bmatrix} F_1 - a_1 F_2 Z - F_4 & -a_1 F_2 P & 0 & -\tau P \\ \frac{a_2 F_2 Z}{1+b_1 P} & a_2 F_2 P - F_3 & \frac{-a_3 Z}{1+b_2 Z} & 0 \\ 0 & 0 & \frac{a_4 Z}{1+b_2 Z} - d_3 & 0 \\ \gamma T & 0 & 0 & \gamma P - d_4 \end{bmatrix},$$

where

$$F_1 = r \ln \left( \frac{K}{P} \right), \quad F_3 = 2e_1 Z + d_2,$$

$$F_2 = \frac{1-\rho}{1+b_1 P}, \quad F_4 = r + d_1 + \tau T.$$

And

$$\lambda_3 = \frac{a_4 Z}{(1+b_2 Z)} - d_3,$$

$\lambda_3 < 0$  if  $a_4 Z < d_3(1+b_2 Z)$ . And other three eigen values are given by the following cubic equation:

$$A_2 \lambda^3 + B_2 \lambda^2 + C_2 \lambda + D_2 = 0,$$

where

$$A_2 = 1 + b_1 P,$$

$$B_2 = (1 + b_1 P)(F_1 + F_3 + F_4 + d_4 - \gamma P - a_2 F_2 P + a_1 F_2 Z),$$

$$C_2 = (F_3 + F_4 - F_1)(d_4 - \gamma P + b_1 d_4 P - b_1 \gamma P^2) + [F_3(F_4 - F_1) + a_2 F_2 P(F_1 - F_4 - d_4) + a_1 F_2 Z(F_3 - \gamma P + d_4)](1 + b_1 P) + b_1 \gamma P^2(a_2 F_2 + \tau T) - a_1 a_2 b_1 F_2^2 P^2 Z,$$

$$D_2 = (F_4 - F_1)(1 + b_1 P)[F_3(d_4 - \gamma P) - a_2 F_2 P(a_4 - \gamma P)] - \gamma \tau P^2 T(a_2 F_2 - b_1 F_3) - a_1 b_1 F_2 P Z(F_3 - a_2 F_2 P)(\gamma P - d_4) + a_1 d_4 F_2 F_3 Z - \gamma \tau P T(a_2 b_1 F_2 P^2 - F_3).$$

According to the Routh-Hurwitz criterion, the equation is asymptotically stable if it satisfies the conditions:  $A_2, B_2, D_2 > 0$  and  $B_2 C_2 - A_2 D_2 > 0$ . Here

- i.  $A_2 > 0, B_2 > 0$  if  $F_1 + F_3 + F_4 + d_4 + a_1 F_2 Z > \gamma P + a_2 F_2 P$ .
- ii.  $D_2 > 0$  if  $F_1 < F_4, a_2 F_2 P(a_4 - \gamma P) < F_3(d_4 - \gamma P), b_1 F_3 < a_2 F_2, \gamma P < d_4$  or  $a_2 F_2 P < F_3, a_2 b_1 F_2 P^2 < F_3$ .

□

**Remark 4.** In Theorem 6, the ecosystem supports phytoplankton and zooplankton, but fish go extinct. The condition  $a_4 Z < d_3(1+b_2 Z)$  means that fish cannot survive if predation on zooplankton is too weak or their mortality is too high. This reflects a partially degraded ecosystem, where pollution or top-level stress prevents the persistence of top predators, leading to trophic truncation.

**Theorem 7.** The Equilibrium point  $E_3(P, Z, F, T)$  is locally asymptotically stable under certain conditions.

*Proof.* Jacobian matrix of Equilibrium point  $E_3(P, Z, F, T)$  is given by:

$$J = \begin{bmatrix} F_1 - a_1 F_2 Z - F_4 & -a_1 F_2 P & 0 & -\tau P \\ \frac{a_2 F_2 Z}{1+b_1 P} & J_{22} & \frac{-a_3 F_6 Z}{(F_5 + F_6 - 1)^2} & 0 \\ 0 & \frac{a_4 F_5 F}{(F_5 + F_6 - 1)^2} & J_{33} & 0 \\ \gamma T & 0 & 0 & F_8 \end{bmatrix},$$

where

$$J_{22} = \frac{a_3 b_2 Z F}{(F_5 + F_6 - 1)^2} + a_2 F_2 P - \frac{a_3 F}{F_5 + F_6 - 1} - F_3,$$

$$J_{33} = \frac{a_4 Z}{F_5 + F_6 - 1} - \frac{a_4 c_2 Z F}{(F_5 + F_6 - 1)^2} - F_7,$$

$$F_1 = r \ln \left( \frac{K}{P} \right), \quad F_2 = \frac{1-\rho}{1+b_1 P}, \quad F_3 = 2e_1 Z + d_2,$$

$$F_4 = r + d_1 + \tau T, \quad F_5 = 1 + c_2 F, \quad F_6 = 1 + b_2 Z,$$

$$F_7 = 2e_2 F + d_3, \quad F_8 = \gamma P - d_4.$$

The eigen values of the above Jacobian matrix are given by the equation:

$$A_3 \lambda^4 + B_3 \lambda^3 + C_3 \lambda^2 + D_3 \lambda + E_3 = 0, \quad (6)$$

where

$$A_3 = (1 + b_1 P)(F_5 + F_6 - 1)^4,$$

$$B_3 = (1 + b_1 P)(F_5 + F_6 - 1)^4(F_4 + a_1 F_2 Z - F_1 - F_8 - J_{22} - J_{33}),$$

$$C_3 = a_1 a_2 F_2^2 P Z (F_5 + F_6 - 1)^4 - a_3 a_4 F_5 F_6 Z F (1 + b_1 P) + (F_5 + F_6 - 1)^4 (1 + b_1 P) [\gamma \tau P T + F_8 (F_1 - F_4 - a_1 F_2 Z) + J_{22} J_{33}] + (F_5 + F_6 - 1)^4 (1 + b_1 P) (F_8 + F_1 - a_1 F_2 Z - F_4) (J_{22} + J_{33}),$$

$$D_3 = J_{22} J_{33} (F_4 + a_1 F_2 Z - F_8 - F_1) (1 + b_1 P) (F_5 + F_6 - 1)^4$$

$$\begin{aligned}
 & + (J_{22} + J_{33})[F_8(F_4 + a_1 F_2 Z - F_1) - \gamma \tau P T](1 \\
 & + b_1 P)(F_5 + F_6 - 1)^4 + a_3 a_4 F_5 F_6 Z F(F_4 + a_1 F_2 Z \\
 & - F_8 - F_1)(1 + b_1 P) + a_1 a_2 F_2^2 P Z(F_8 + J_{33})(F_5 \\
 & + F_6 - 1)^4, \\
 E_3 = & J_{22} J_{33}[F_8(F_1 - F_4 - a_1 F_2 Z) + \gamma \tau P T](1 + b_1 P)(F_5 \\
 & + F_6 - 1)^4 + a_3 a_4 F_5 F_6 Z F(1 + b_1 P)[\gamma \tau P T + F_8(F_1 \\
 & - a_1 F_2 Z - F_4)] + a_1 a_2 F_2^2 F_8 J_{33} P Z(F_5 + F_6 - 1)^4.
 \end{aligned}$$

According to the Routh-Hurwitz criterion, the equation is asymptotically stable if it satisfies the conditions:  $A_3, B_3, C_3, D_3, E_3 > 0, A_3 D_3 - B_3 C_3 > 0, A_3 D_3^2 - B_3 C_3 D_3 - B_3^2 E_3 > 0$ .

- $A_3 > 0, B_3 > 0$  if,  $F_1 + F_8 + J_{22} + J_{33} < F_4 + a_1 F_2 Z$ ,
- $C_3 > 0, D_3 > 0, E_3 > 0$  if,  $a_3 a_4 F_5 F_6 F < a_1 a_2 F_2^2 P$ ,  $F_1 + F_8 < a_1 F_2 Z + F_4, F_4 + a_1 F_2 Z < F_1$ .

□

**Remark 5.** Theorem 7 indicates that all species coexist stably when ecological interactions (like predator interference and intraspecific competition) are strong enough to counteract destabilizing effects of predation and toxicants. The balance among growth, consumption, and decay prevents large oscillations. Instability here would mean population fluctuations or collapse due to imbalance, such as excessive toxicant accumulation or weak self-regulation.

## 6. Global Stability

In this section, we establish the global stability of the equilibrium point  $E_3(P, Z, F, T)$  within the bounded region  $\Omega$ . By constructing a suitable Lyapunov function and applying Sylvester's criteria, we derive sufficient conditions under which the system converges globally to this equilibrium. The following theorem presents the necessary conditions for global asymptotic stability.

**Theorem 8.** In the region  $\Omega$ , if the following conditions hold:

$$a_2(1 - \rho)b_1\bar{Z} < r\sigma_2, \quad (7)$$

$$a_3b_2\bar{F} < e_1\sigma_1 \quad (8)$$

$$\gamma\bar{P} < d_4, \quad (9)$$

$$\sigma_2\gamma^2T^2 < (r\sigma_2 - a_1(1 - \rho)b_1\bar{Z})(\gamma\bar{P} - d_4), \quad (10)$$

where

$$\sigma_1 = (1 + b_2Z + c_2F)(1 + b_2\bar{Z} + c_2\bar{F}),$$

$$\sigma_2 = (1 + b_1P)(1 + b_1\bar{P}),$$

$$A_1 = \frac{a_1(1 + b_1\bar{P})}{a_2} > 0,$$

$$A_2 = \frac{a_1a_3(1 + b_1\bar{P})(1 + b_2\bar{Z})}{a_2a_4(1 + c_2\bar{F})} > 0,$$

$$A_3 = 1.$$

Then  $E_3(P, Z, F, T)$  will be globally asymptotically stable in the

region  $\Omega$ .

*Proof.* Let us consider,

$$\begin{aligned}
 V_{11} = & \left[ P - \bar{P} - \bar{P} \ln \left( \frac{P}{\bar{P}} \right) \right] + A_1 \left[ Z - \bar{Z} - \bar{Z} \ln \left( \frac{Z}{\bar{Z}} \right) \right] \\
 & + A_2 \left[ F - \bar{F} - \bar{F} \ln \left( \frac{F}{\bar{F}} \right) \right] + \frac{A_3}{2} (T - \bar{T})^2.
 \end{aligned}$$

Differentiating both side with respect to  $t$ , we get,

$$\begin{aligned}
 \frac{dV_{11}}{dt} = & \left( \frac{P - \bar{P}}{P} \right) \frac{dP}{dt} + A_1 \left( \frac{Z - \bar{Z}}{Z} \right) \frac{dZ}{dt} + A_2 \left( \frac{F - \bar{F}}{F} \right) \frac{dF}{dt} \\
 & + A_3(T - \bar{T}) \frac{dT}{dt}.
 \end{aligned}$$

From eqs. (1) to (4), we get,

$$\begin{aligned}
 \frac{dV_{11}}{dt} = & r(-\ln P + \ln \bar{P})(P - \bar{P}) + \frac{a_1(1 - \rho)b_1\bar{Z}}{\sigma_2}(P - \bar{P})^2 \\
 & - \frac{(1 - \rho)}{\sigma_2} (a_1(1 + b_1\bar{P}) - a_2A_1)(P - \bar{P})(Z - \bar{Z}) \\
 & + A_1 \left( \frac{a_3b_2\bar{F}}{\sigma_1} - e_1 \right) (Z - \bar{Z})^2 - A_2 \left( e_2 + \frac{a_4c_2\bar{Z}}{\sigma_1} \right) (F \\
 & - \bar{F})^2 + A_3(\gamma\bar{P} - d_4)(T - \bar{T})^2 + A_3\gamma T(P - \bar{P}) \\
 & (T - \bar{T}) - \frac{1}{\sigma_1} (a_3A_1(1 + b_2\bar{Z}) - a_4A_2(1 + c_2\bar{F})X) (Z \\
 & - \bar{Z})(F - \bar{F}),
 \end{aligned}$$

where

$$\sigma_1 = (1 + b_2Z + c_2F)(1 + b_2\bar{Z} + c_2\bar{F}),$$

$$\sigma_2 = (1 + b_1P)(1 + b_1\bar{P}),$$

and choosing

$$A_1 = \frac{a_1(1 + b_1\bar{P})}{a_2} > 0,$$

$$A_2 = \frac{a_1a_3(1 + b_1\bar{P})(1 + b_2\bar{Z})}{a_2a_4(1 + c_2\bar{F})} > 0,$$

$$A_3 = 1.$$

Since  $-\ln P + \ln \bar{P} < -(P - \bar{P}) \quad \forall P > 0$ , then  $\frac{dV_{11}}{dt}$  can be written as:

$$\begin{aligned}
 \frac{dV_{11}}{dt} \leq & - \left[ \frac{b_{11}}{2} (P - \bar{P})^2 + b_{14} (P - \bar{P})(T - \bar{T}) + \frac{b_{44}}{2} (T - \bar{T})^2 \right. \\
 & \left. + b_{22} (Z - \bar{Z})^2 + b_{33} (F - \bar{F})^2 \right],
 \end{aligned}$$

where

$$b_{11} = r - \frac{a_1b_1(1 - \rho)\bar{Z}}{\sigma_2},$$

$$b_{22} = A_1 \left( e_1 - \frac{a_3b_2\bar{F}}{\sigma_1} \right),$$

$$b_{33} = A_2 \left( e_2 + \frac{a_4c_2\bar{Z}}{\sigma_1} \right),$$

$$b_{44} = A_3 (d_4 - \gamma\bar{P}),$$



$$b_{14} = -A_3\gamma T.$$

By the Sylvester's criteria, we get that  $\frac{dv_{11}}{dt}$  will be negative function with the inequalities:

$$b_{11} > 0, \quad (11)$$

$$b_{22} > 0, \quad (12)$$

$$b_{44} > 0, \quad (13)$$

$$b_{11}b_{44} > b_{14}^2. \quad (14)$$

We note that the inequalities, eq. (7)  $\Rightarrow$  eq. (11), eq. (8)  $\Rightarrow$  eq. (12), eq. (9)  $\Rightarrow$  eq. (13), and eq. (10)  $\Rightarrow$  eq. (14). Hence  $V_{11}$  of  $E_3$  in  $\Omega$ . Prove theorem.  $\square$

**Remark 6.** The conditions of Theorem 8 ensure that toxicant levels are sufficiently controlled, and that predation and competition are balanced. When they hold, the system always converges to a biologically viable state with coexistence of all populations, regardless of initial values. Ecologically, this suggests that the ecosystem is resilient to perturbations provided that pollution remains within safe limits and population interactions are properly regulated.

## 7. Bifurcation Analysis

In this section, we investigate the occurrence of a Hopf bifurcation by identifying purely imaginary eigenvalues and verifying stability changes using the Routh-Hurwitz criteria. Additionally, we confirm the transversality condition through Sotomayor's theorem.

**Theorem 9.** The system eqs. (1) to (4) undergoes a Hopf bifurcation at the equilibrium point  $E_1(P, 0, 0, T)$  as the parameter  $K$  crosses the critical threshold

$$K_c = P \exp \left[ \frac{1}{r} \left( \frac{\tau S}{d_4 - \gamma P} - \gamma P + r + d_1 + d_4 \right) \right],$$

provided that the following condition holds at  $K = K_c$ :

$$(\tau T - \gamma P + d_4)(\gamma P - d_4) + \tau d_4 T > 0.$$

*Proof.* For a Hopf bifurcation to occur, the trace of the eq. eq. (5) must be zero, i.e.,  $A_1 = 0$ .

Solving for  $K$ , we obtain,

$$K_c = P \exp \left[ \frac{1}{r} (\tau T - \gamma P + r + d_1 + d_4) \right].$$

Substituting the value of  $T$  from Theorem 2, we obtain,

$$K_c = P \exp \left[ \frac{1}{r} \left( \frac{\tau S}{d_4 - \gamma P} - \gamma P + r + d_1 + d_4 \right) \right].$$

Now  $B_1 > 0$

$$\left( r \ln \left( \frac{K}{P} \right) - r - d_1 \right) (\gamma P - d_4) + \tau d_4 T > 0,$$

substituting  $K = K_c$  when  $A_1 = 0$ , we obtain,

$$(\tau T - \gamma P + d_4)(\gamma P - d_4) + \tau d_4 T > 0.$$

Now,

$$\frac{dA_1}{dK} = \frac{-r}{K_c} \neq 0,$$

Since this condition is satisfied, the transversality requirement of Sotomayor's Theorem for Hopf Bifurcation holds, confirming the bifurcation.  $\square$

**Remark 7.** The Hopf bifurcation at  $E_1$  implies that when the carrying capacity  $K$  exceeds the critical value  $K_c$ , the equilibrium loses stability, and the system exhibits oscillatory behavior. Biologically, this reflects that the phytoplankton population, in the absence of consumers, begins to fluctuate periodically due to increased resource availability.

## 8. Numerical Simulation

In this section, we conduct a comprehensive stability analysis of the equilibria  $E_1, E_2$ , and  $E_3$  by computing eigenvalues and confirming stability conditions. A Hopf bifurcation analysis at  $E_1$  is performed to determine critical thresholds for oscillatory behavior. Furthermore, the impact of toxicant accumulation on population dynamics is examined, along with the effects of varying key ecological parameters. Using MATLAB, bifurcation diagrams and phase trajectories are generated to illustrate stability transitions and long-term system behavior under different parameter settings.

### 8.1. Stability Analysis

The parameters used in this study are assumed to reflect general ecological conditions of an aquatic food chain. Although not derived from specific empirical datasets, they were selected to ensure biological feasibility, the existence of positive equilibria, and ecologically meaningful species interactions. The values are chosen to represent a realistic trophic structure, where phytoplankton serve as the resource base for zooplankton, which in turn support fish populations. The resulting equilibrium values maintain the expected biomass hierarchy (phytoplankton > zooplankton > fish) in terms of population density, aligning with commonly observed patterns in aquatic ecosystems.

**Example 1.** To illustrate the stability of the equilibrium point  $E_1(P, 0, 0, T)$ , we consider the system eqs. (1) to (4) with the following parameter values:

$$\begin{array}{lll} r = 5, & K = 15, & a_1 = 0.35, \\ \rho = 0.4, & b_1 = 0.1, & d_1 = 0.012, \\ \tau = 1.5, & a_2 = 0.01, & a_3 = 0.9, \\ b_2 = 0.1, & c_2 = 0.05, & d_2 = 0.2, \\ e_1 = 0.005, & a_4 = 0.3, & d_3 = 0.8, \\ e_2 = 0.12, & S = 0.8, & d_4 = 0.5, \\ \gamma = 0.03. \end{array}$$

For these parameter values, one of the equilibrium points is

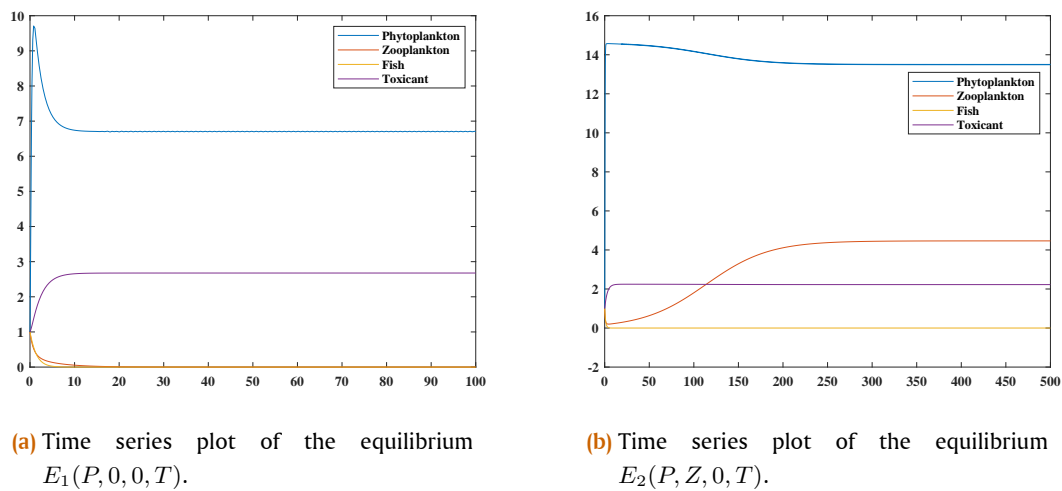


**Figure 1.** Note: The x-axis represents time in arbitrary units, and the y-axis represents relative population density. These values are not associated with specific field data but illustrate qualitative system behavior.

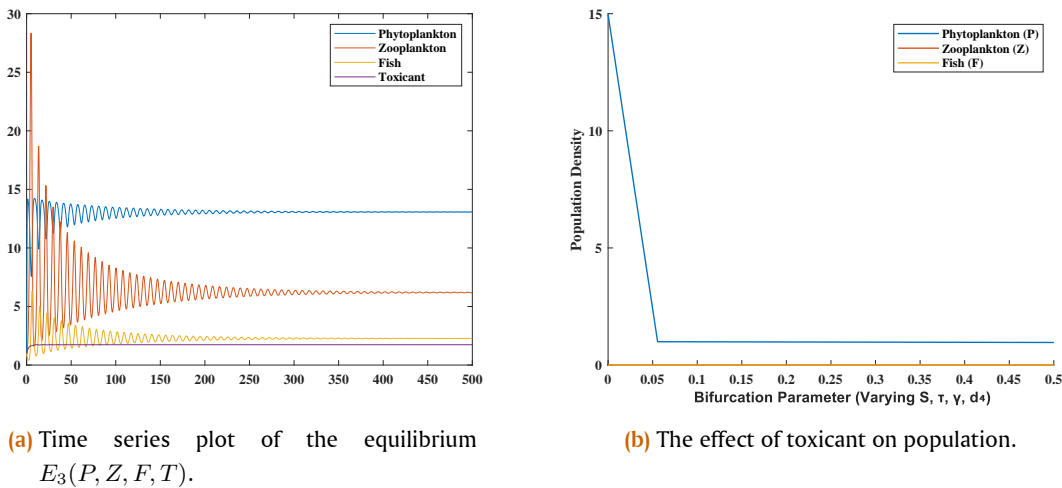


**Figure 2.** Note: The x-axis represents time in arbitrary units, and the y-axis represents relative population density. These values are not associated with specific field data but illustrate qualitative system behavior.

found at:

$$E_1(6.7102, 0.0000, 0.0000, 2.6765).$$

To analyze the stability of this equilibrium, we compute the eigenvalues of the Jacobian matrix at  $E_1$ , which are:

$$\begin{aligned} \lambda_1 &= -4.8228, & \lambda_2 &= -0.4774, \\ \lambda_3 &= -0.1759, & \lambda_4 &= -0.8000. \end{aligned}$$

Since all eigenvalues have negative real parts, the equilibrium point  $E_1$  is locally asymptotically stable. This is further supported by the time series simulation in Figure 1a, which shows the system smoothly converging to equilibrium without oscillations after a small perturbation.

**Example 2.** To illustrate the stability of the equilibrium point  $E_2(P, Z, 0, T)$ , we consider the system eqs. (1) to (4) with the following parameter values:

$$\begin{aligned} r &= 5, & K &= 15, & a_1 &= 0.35, \\ \rho &= 0.4, & b_1 &= 0.1, & d_1 &= 0.12, \\ \tau &= 0.004, & a_2 &= 0.05, & a_3 &= 1.7, \\ b_2 &= 0.1, & c_2 &= 0.05, & d_2 &= 0.15, \\ e_1 &= 0.005, & a_4 &= 0.3, & d_3 &= 1, \\ e_2 &= 0.12, & S &= 0.8, & d_4 &= 0.4, \\ \gamma &= 0.003. \end{aligned}$$

For these parameter values, one of the equilibrium points is found at:

$$E_2(13.5028, 4.4647, 0.0000, 2.2252).$$

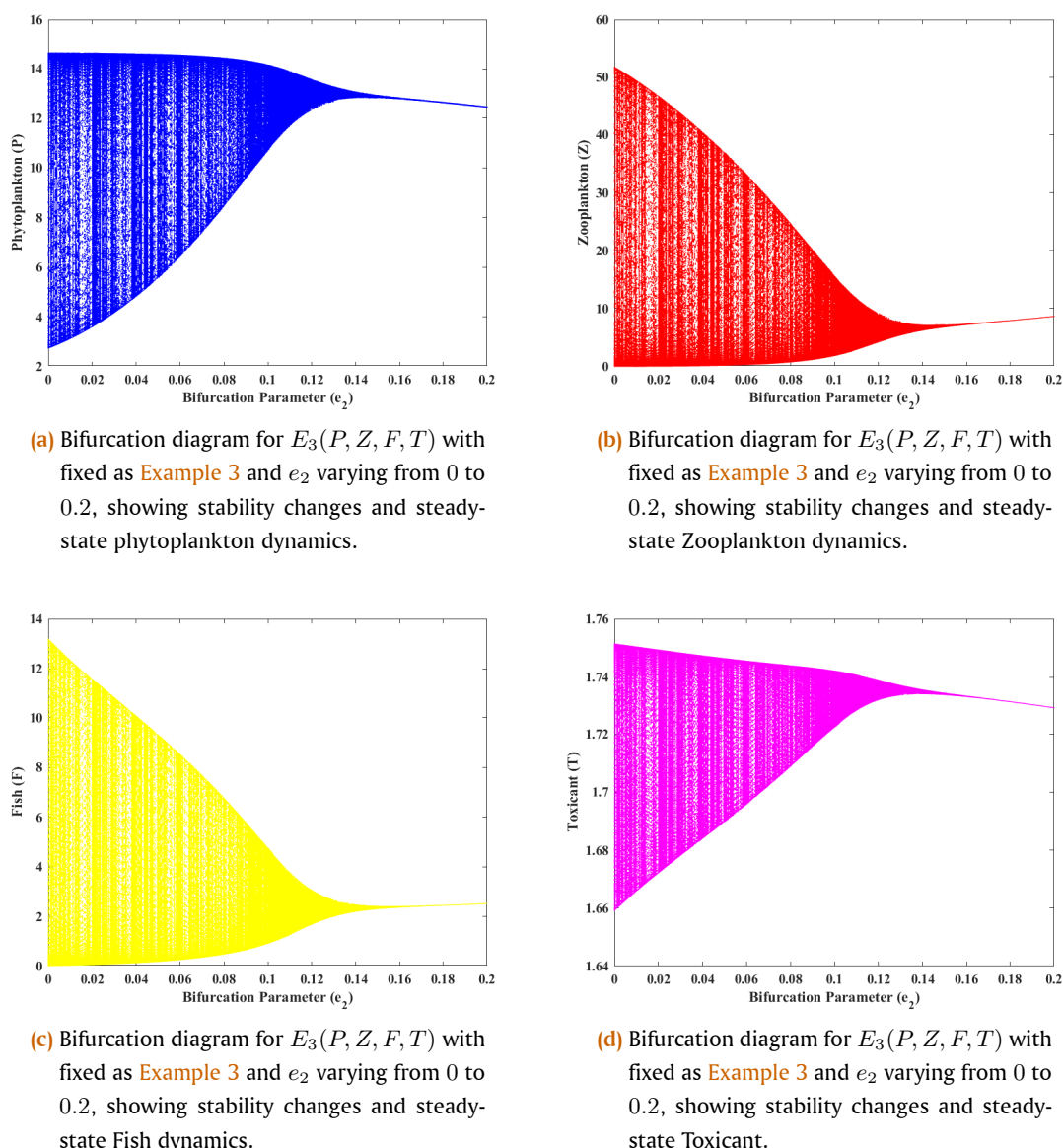


Figure 3.

To analyze the stability of this equilibrium, we compute the eigenvalues of the Jacobian matrix at  $E_2$ , which are:

$$\begin{aligned}\lambda_1 &= -4.7666, & \lambda_2 &= -0.0285, \\ \lambda_3 &= -0.4596, & \lambda_4 &= -0.0740.\end{aligned}$$

Since all eigenvalues have negative real parts, the equilibrium point  $E_2$  is locally asymptotically stable. This is further supported by the time series simulation in Figure 1b, which shows the system smoothly converging to equilibrium without oscillations after a small perturbation.

**Example 3.** To illustrate the stability of the equilibrium point  $E_3(P, Z, F, T)$ , we consider the system eqs. (1) to (4) with

the following parameter values:

$$\begin{aligned}r &= 5, & K &= 15, & a_1 &= 0.35, \\ \rho &= 0.4, & b_1 &= 0.1, & d_1 &= 0.12, \\ \tau &= 0.003, & a_2 &= 0.4, & a_3 &= 0.9, \\ b_2 &= 0.1, & c_2 &= 0.05, & d_2 &= 0.15, \\ e_1 &= 0.005, & a_4 &= 0.3, & d_3 &= 0.8, \\ e_2 &= 0.12, & S &= 0.8, & d_4 &= 0.4, \\ \gamma &= 0.003.\end{aligned}$$

For these parameter values, one of the equilibrium points is found at:

$$E_3(13.0851, 6.1811, 2.2632, 1.7362).$$

To analyze the stability of this equilibrium, we compute the

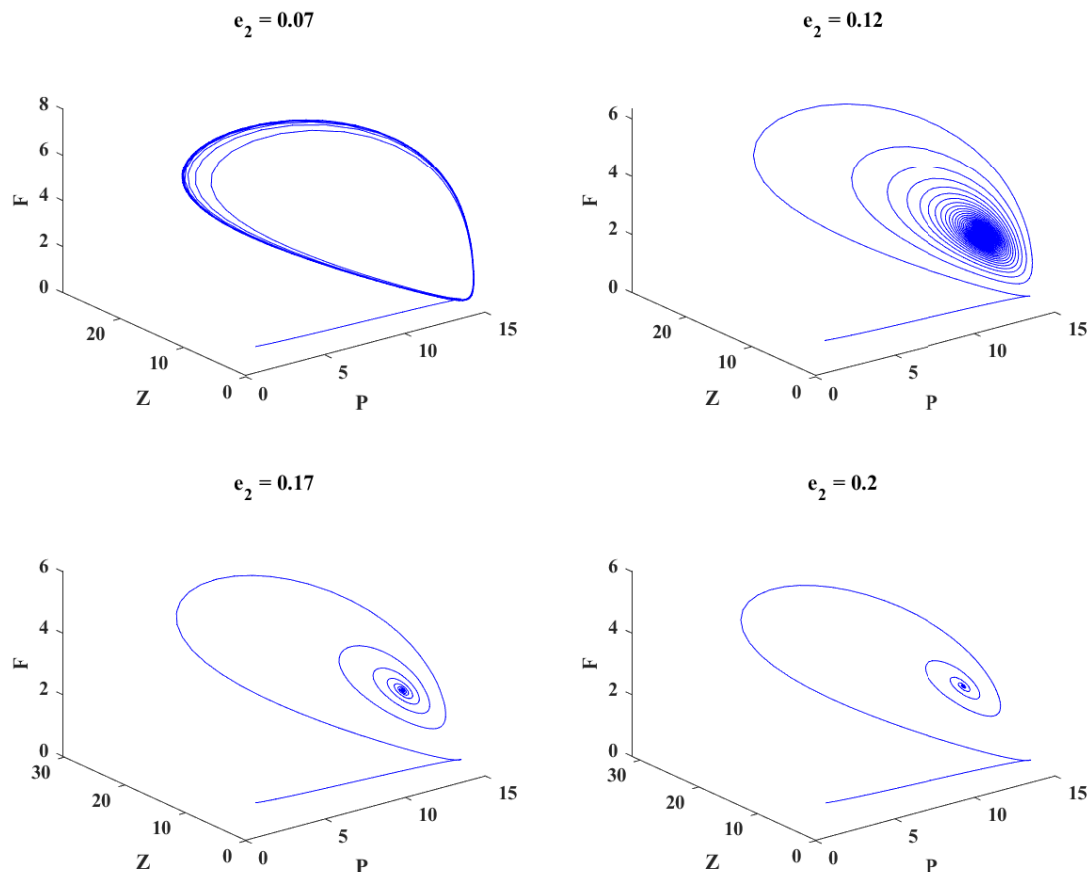


**Figure 4.** 3D phase trajectories for equilibrium point  $E_3(P, Z, F, T)$  with  $e_2 = 0.07, 0.12, 0.17, 0.2$ , showing system dynamics while all other parameters remain fixed as in [Example 3](#).

eigenvalues of the Jacobian matrix at  $E_3$ , which are:

$$\begin{aligned} \lambda_1 &= -4.6220, & \lambda_2 &= -0.0069 + 0.8101i, \\ \lambda_3 &= -0.0069 - 0.8101i, & \lambda_4 &= -0.4608. \end{aligned}$$

Since all eigenvalues have negative real parts, the equilibrium point  $E_3$  is locally asymptotically stable. This is further supported by the time series simulation in [Figure 2a](#), which shows the system converging to equilibrium after oscillations.

## 8.2. Effect of Toxicant on Population

The bifurcation analysis in [Figure 2b](#) demonstrates how changes in toxicant-related parameters ( $S, \tau, \gamma, d_4$ ) influence the populations of phytoplankton, zooplankton, and fish. As the toxicant input  $S$  or its effects ( $\tau, \gamma$ ) increase, phytoplankton populations decline significantly. This reduction disrupts the food supply for zooplankton, causing their population to approach near extinction. Consequently, fish, which rely on zooplankton for sustenance, also experience a drastic decline, leading to a collapse in the entire food chain. These findings underscore the destabilizing effects of toxicant accumulation in aquatic ecosystems, potentially driving species to extinction at high toxicity lev-

els. The results align with real-world scenarios where pollution and industrial runoff severely impact aquatic food chains, highlighting the importance of regulating toxicant levels to maintain ecological balance.

## 8.3. Hopf-Bifurcation Analysis

To investigate the occurrence of a Hopf bifurcation, we vary the carrying capacity  $K$ , while taking other parameter from [Example 1](#) and compute the equilibrium states and their stability. From [Theorem 9](#), a Hopf bifurcation occurs when the trace of the Jacobian matrix is zero. Solving for  $K$ , we obtain the critical value  $K_c = 43.2859$ . At this bifurcation point, the equilibrium shifts to:

$$E_1 = (6.7038, 0, 0, 2.6766).$$

The eigenvalues of the Jacobian matrix at  $K_c$  are:

$$\begin{aligned} \lambda_1 &= 0.8474i, & \lambda_2 &= -0.8474i, \\ \lambda_3 &= -0.1759, & \lambda_4 &= -0.8000. \end{aligned}$$

The presence of purely imaginary eigenvalues ( $\pm 0.8474i$ ) confirms the onset of a Hopf bifurcation.

Verification of the Transversality Condition: For the Hopf bifurcation to occur, the transversality condition must hold:

$$\frac{dA_1}{dK} = -0.11551 \neq 0.$$

Since this value is nonzero, the transversality condition is satisfied, confirming the existence of a Hopf bifurcation.

- For  $K < K_c$ , the equilibrium  $E_1$  remains stable, and the system converges to a steady state.
- For  $K > K_c$ , the equilibrium loses stability.

#### 8.4. Effect of $e_2$ on System Dynamics

The bifurcation analysis of  $e_2$  is conducted by varying its value from 0 to 0.2 while keeping all other parameters fixed. The bifurcation diagrams Figures 3a to 3d illustrate that for small values of  $e_2$ , the system exhibits chaotic or quasi-periodic oscillations, leading to irregular fluctuations in phytoplankton, zooplankton, fish, and toxicant populations. As  $e_2$  increases beyond  $e_2 \approx 0.12$ , oscillations begin to dampen, and periodic behavior emerges. Beyond  $e_2 \approx 0.15$ , the system transitions to a stable equilibrium, where all populations settle into steady-state values. The phase trajectories Figure 4 confirm this transition, showing large periodic orbits at lower  $e_2$  values, which shrink and spiral inward as  $e_2$  increases, ultimately converging to a fixed equilibrium at  $e_2 = 0.2$ . This analysis highlights the stabilizing effect of  $e_2$ , as higher values suppress oscillatory dynamics across all species and promote equilibrium.

### 9. Discussion

This study develops a mathematical model to describe the interactions within an aquatic ecosystem, incorporating key ecological mechanisms such as Gompertz growth, prey refuge, Holling Type II predation, and the Beddington–DeAngelis functional response. By integrating these elements, the model provides valuable insights into population stability and bifurcation behavior.

Boundedness conditions were established to ensure biological feasibility, and upper limits for all populations were derived. The existence and stability of equilibria  $E_1$ ,  $E_2$ , and  $E_3$  were examined using the Jacobian matrix and Routh–Hurwitz criteria, with global stability confirmed through a Lyapunov function. Numerical simulations further validated equilibrium stability across various parameter settings.

Hopf bifurcation analysis at  $E_1$  was conducted both theoretically and numerically by varying the carrying capacity  $K$ . A critical threshold  $K_c = 43.2859$  was identified, leading to an equilibrium shift to  $E_1(6.7038, 0, 0, 2.6766)$ . The emergence of purely imaginary eigenvalues  $\pm 0.8474i$  at  $K_c$  confirmed the occurrence of a Hopf bifurcation. The transversality condition was satisfied, ensuring the bifurcation's validity. For  $K < K_c$ ,  $E_1$  remained stable, while for  $K > K_c$ , it became unstable, demonstrating the influence of carrying capacity on population dynamics. Biologically, the Hopf bifurcation indicates that as  $K$  increases beyond the critical value, the system transitions from a stable equilibrium to oscillatory dynamics. This suggests that phytoplankton and toxicant levels may begin to fluctuate cyclically rather than stabilize.

Bifurcation analysis of  $E_3$  with respect to  $e_2$  revealed a transition from chaotic or quasi-periodic oscillations to a stable equilibrium as  $e_2$  increased beyond approximately 0.15. Phase trajectory analysis showed that higher intraspecific competition among fish reduces oscillatory behavior and promotes steady-state dynamics. This emphasizes the stabilizing role of self-

regulation at the top trophic level.

The study also highlights the detrimental impact of toxicant accumulation on the aquatic food chain. Increasing toxicant-related parameters ( $S, \tau, \gamma, d_4$ ) leads to a decline in phytoplankton, which disrupts energy transfer to higher trophic levels. As a result, zooplankton populations decline significantly, causing a subsequent collapse in fish populations. This destabilization underscores the importance of managing toxicant levels to maintain ecological balance and prevent species extinction.

The results of this study provide valuable insights for ecological management. Regulating key parameters such as carrying capacity and toxicant input can help prevent system destabilization, highlighting the importance of environmental interventions in sustaining population balance and ecosystem stability. While the current model captures essential ecological interactions, it assumes a spatially homogeneous environment and constant parameter values. To enhance ecological realism, potential extensions of the model could incorporate spatial diffusion to reflect species movement, stochastic effects to capture environmental variability, and seasonal forcing to account for periodic ecological changes. Additionally, empirical validation using field or laboratory data on toxicant concentrations and species densities would increase the model's practical relevance and support its application in ecosystem risk assessment.

It is also important to note that the model assumes homogeneous mixing, constant parameter values, and no age or spatial structure. These simplifications enable analytical tractability but may limit the quantitative accuracy of predictions in real ecosystems. Accordingly, the results should be interpreted as qualitative insights that offer a theoretical foundation for more detailed ecological modeling and future empirical investigation.

**Author Contributions.** Annavarapu, R. B.: Conceptualization, Methodology. Makwana, K.: Formulation of the mathematical model, Mathematical analysis, Numerical Simulations, Software Implementation, Writing-original draft preparation, Data Visualization (graphs). Jadon, B. P. S.: Supervision.

**Acknowledgement.** The authors sincerely thank the editors and reviewers for their valuable feedback, which has helped improve the manuscript. We also appreciate the insightful discussions and guidance from our colleagues and mentors during this work.

**Funding.** This research received no external funding.

**Conflict of interest.** The authors declare no conflict of interest.

**Data availability.** Not applicable.

### References

- [1] R. P. Kaur *et al.*, "Chaos control of chaotic plankton dynamics in the presence of additional food, seasonality, and time delay," *Chaos, Solitons and Fractals*, vol. 153, no. 1, p. 111521, 2021. DOI:10.1016/j.chaos.2021.111521
- [2] P. Panja, "Dynamics of a Plankton-Fish Model with Infection in Phytoplankton Species," *Journal of Applied Nonlinear Dynamics*, vol. 12, no. 4, pp. 689–706, 2023. DOI:10.5890/JAND.2023.12.005
- [3] N. K. Thakur *et al.*, "Modeling the plankton–fish dynamics with top predator interference and multiple gestation delays," *Nonlinear Dynamics*, vol. 100, no. 4, pp. 4003–4029, 2020. DOI:10.1007/s11071-020-05688-2
- [4] R. B. Annavarapu, K. Yadav, and B. P. S. Jadon, "The study of top predator interference on tri species with "food-limited" model under the toxicant



- environment: A mathematical implication," *Liberte Journal*, vol. 13, no. 1, pp. 20–35, 2025. DOI:10.14118.LRJ.2025.V13I1.485462
- [5] S. S. Obonin, U. C. Amadi, and K. S. Sylvanus, "The Effects of External Toxicants on Competitive Environment: A Mathematical Modeling Approach," *Communication in Physical Sciences*, vol. 11, no. 4, pp. 852–863, 2024.
- [6] N. Zhang, Y. Kao, and B. Xie, "Impact of fear effect and prey refuge on a fractional order prey–predator system with Beddington–DeAngelis functional response," *Chaos*, vol. 32, no. 4, pp. 1–17, 2022. DOI:10.1063/5.0082733
- [7] Y. Shao and W. Kong, "A Predator–Prey Model with Beddington–DeAngelis Functional Response and Multiple Delays in Deterministic and Stochastic Environments," *Mathematics*, vol. 10, no. 18, p. 3378, 2022. DOI:10.3390/math10183378
- [8] X. Y. Meng and J. G. Wang, "Analysis of a delayed diffusive model with Beddington–DeAngelis functional response," *International Journal of Biomathematics*, vol. 12, no. 4, p. 1950047, 2019. DOI:10.1142/s1793524519500475
- [9] E. Rahmi *et al.*, "A Modified Leslie–Gower Model Incorporating Beddington–DeAngelis Functional Response, Double Allee Effect and Memory Effect," *Fractal and Fractional*, vol. 5, no. 3, p. 84, 2021. DOI:10.3390/fractalfract5030084
- [10] S. Yu and F. Chen "Dynamic Behaviors of a Competitive System with Beddington–DeAngelis Functional Response," *Discrete Dynamics in Nature and Society*, vol. 2019, pp. 1–12, 2019. DOI:10.1155/2019/4592054
- [11] M. Mukherjee *et al.*, "Prey–predator optimal harvesting mathematical model in the presence of toxic prey under interval uncertainty," *Scientific African*, vol. 21, p. e01837, 2023. DOI:10.1016/j.sciaf.2023.e01837
- [12] M. Zhu and H. Xu, "Dynamics of a delayed reaction-diffusion predator-prey model with the effect of the toxins," *Mathematical Biosciences and Engineering*, vol. 20, no. 4, pp. 6894–6911, 2023. DOI:10.3934/mbe.2023297
- [13] S. N. Majeed and R. K. Naji, "Dynamical Behavior of Two Predators-One Prey Ecological System with Refuge and Beddington –De Angelis Functional Response," *Iraqi Journal of Science*, vol. 64, no. 12, pp. 6383–6400, 2023. DOI:10.24996/ij.s.2023.64.12.24
- [14] Z. Lajmiri, I. Orak, and S. Hosseini, "Dynamics of a predator-prey system with prey refuge," *Computational Methods for Differential Equations*, vol. 7, no. 3, pp. 454–474, 2019.
- [15] F. S. Berezovskaya, B. Song, and C. Castillo-Chavez, "Role of Prey Dispersal and Refuges on Predator-Prey Dynamics," *SIAM Journal on Applied Mathematics*, vol. 70, no. 6, pp. 1821–1839, 2010. DOI:10.1137/080730603
- [16] O. P. Misra and R. B. Annavarapu, "Modelling effect of toxicant in a three-species food-chain system incorporating delay in toxicant uptake process by prey," *Modeling Earth Systems and Environment*, vol. 2, no. 77, pp. 1–27, 2016. DOI:10.1007/s40808-016-0128-4
- [17] O. P. Misra and R. B. Annavarapu, "Mathematical study of a Leslie–Gower-type tritrophic population model in a polluted environment," *Modeling Earth Systems and Environment*, vol. 2, no. 1, p. 29, 2016. DOI:10.1007/s40808-016-0084-z
- [18] P. K. Santra, "Discrete-time prey-predator model with  $\theta$  -logistic growth for prey incorporating square root functional response," *Jambura Journal of Biomathematics (JJBM)*, vol. 1, no. 2, pp. 41–48, 2020. DOI:10.34312/jjbm.v1i2.7660
- [19] R. Ahmed and M. B. Almatraf, "Complex Dynamics of a Predator-Prey System With Gompertz Growth and Herd Behavior," *International journal of Analysis and Applications*, vol. 21, p. 100, 2023. DOI:10.28924/2291-8639-21-2023-100
- [20] S. Md. S. Rana, "Dynamic complexity in a discrete-time predator-prey system with Holling type I functional response: Gompertz growth of prey population," *Computational Ecology and Software*, vol. 10, no. 4, pp. 200–216, 2020.
- [21] C. Liu *et al.*, "Bifurcation and Stability Analysis of a New Fractional-Order Prey–Predator Model with Fear Effects in Toxic Injections," *Mathematics*, vol. 11, no. 20, p. 4367, 2023. DOI:10.3390/math11204367
- [22] S. Bosi and D. Desmarchelier, "Local bifurcations of three and four-dimensional systems: A tractable characterization with economic applications," *Mathematical Social Sciences*, vol. 97, pp. 38–50, 2019. DOI:10.1016/j.mathsocsci.2018.11.001
- [23] N. Wang *et al.*, "Bifurcation Behavior Analysis in a Predator-Prey Model," *Discrete Dynamics in Nature and Society*, vol. 2016, no. 1, pp. 1–11, 2016. DOI:10.1155/2016/3565316
- [24] K. Makwana, R. B. Annavarapu, and B. P. S. Jadon, "Effects of Toxicant on One Prey and Two Competing Predators with Beddington-DeAngelis Functional Response," *Jambura Journal of Biomathematics (JJBM)*, vol. 6, no. 1, pp. 44–59, 2025. DOI:10.37905/jjbm.v6i1.30686
- [25] P. Cong, M. Fan, and X. Zou, "Dynamics of a three-species food chain model with fear effect", *Communications in Nonlinear Science and Numerical Simulation*, vol. 99, p. 105809, 2021. DOI:10.1016/j.cnsns.2021.105809